Dependence of Geometric Magnetic Anisotropy in Thin Iron Films

T. G. KNORR* AND R. W. HOFFMAN
Case Institute of Technology, Cleveland, Ohio
(Received October 7, 1958)

Thin iron films produced by vacuum deposition are observed to display a magnetic anisotropy dependent on the geometric location of the evaporating filament. A fiber axis structure is induced during the evaporation. If the direction of incidence of the metallic flux varies from a normal to the substrate this fiber axis tilts in a similar direction. As soon as the fiber axis is no longer normal to the plane of the film, magnetic anisotropy is produced. The variation of the tilt of the fiber axis correlates with and can be shown to account for the geometric dependence of the observed anisotropy. Calculations of the magnetic anisotropy expected in a film with a fiber axis structure and an anisotropic tensile stress in the plane of the film agree with the experimental observations for those films which show only rotational switching. Anisotropies of 3×10^4 ergs/cm^3 have been observed in iron films about 350 A thick prepared without the use of applied magnetic fields either during deposition or during a subsequent thermal anneal.

INTRODUCTION

THIN ferromagnetic films prepared by vacuum deposition are found to display various types of magnetic anisotropy.[1–6] The authors would like to point out that the references listed here are merely indicative of the work being performed and are in no way intended to be a comprehensive listing. Most of the work has been done in specimens evaporated in a strong magnetic field or subsequently annealed at high temperatures in such a field. These conditions are known to induce uniaxial anisotropy in the films, but the exact reason for this is not, as yet, clearly defined.

Magnetic measurements are taken dynamically in a loop tracer or statically in a torque magnetometer. Anisotropy has also been determined by observing domain walls in the specimen with the familiar "Bitter technique."

In recent years considerable interest in thin ferromagnetic films has developed because of the advantages of employing these films as memory storage units in high-speed computational devices.[7] For this application films possessing a uniaxial anisotropy are desired. Hence, most of these investigations have been performed in films in which such an anisotropy has been induced. An easy direction of magnetization is established parallel to a magnetic field applied during the deposition or during magnetic anneal of the specimens. Observations have indicated that the strength of the field necessary to produce such uniaxial anisotropy in iron films is in the range of a few oersteds if not the earth's field, itself.[2]

In the experiments to be described, the origin of magnetic anisotropy in thin films is in itself studied more extensively than any effects that might arise from such an anisotropy. The films are produced under carefully controlled conditions and the change in anisotropy is observed as these conditions are varied.

EXPERIMENTAL PROCEDURES

The films used in this investigation were formed by vacuum evaporation of iron from hot tungsten filaments. The metal was deposited at a rate of 60 angstrom units per second, on glass substrates held at 75°C. Pressures during the deposition were 1.5×10^{-6} mm of Hg or less, obtained after overnight outgassing of the complete vacuum system and using liquid nitrogen and charcoal trapping during the evaporation. Upon removal from the vacuum system the iron films displayed a bright shiny metallic appearance and have retained this luster for two years. This results from the oxide layer which quickly forms on pure iron as reported by Nelson.[8]

Magnetic measurements were made in a separate 60-cycle loop tracer under normal atmospheric conditions. These measurements were begun as soon after the deposition as possible and within fifteen minutes after the sample was exposed to atmospheric pressure. Nelson reports that an oxide layer about 15 A thick forms rapidly under such conditions and that any further oxidation is negligible. Measurements of the electrical resistivity in this laboratory during the opening of the vacuum system and weeks later agree with Nelson's observations that most of the oxidation occurs immediately upon exposure to atmospheric pressure. Hence, the necessity of exposing the sample to room conditions for the magnetic measurement actually results in a study of iron films covered with a thin layer of oxide. The only effect this oxide layer has on the magnetic properties of the underlying film is a decrease in the film's "magnetic thickness." If the specimen is thin enough, a decrease in the value of the

* Now at the University of Dayton, Dayton, Ohio.
[1] R. L. Conger, Phys. Rev. **98**, 1752 (1955).
[2] M. S. Blois, Jr., J. Appl. Phys. **26**, 975 (1955).
[3] K. Zaveta, Czechoslov. J. Phys. **6**, 473 (1956).
[4] S. Chikazumi and T. Oomura, J. Phys. Soc. Japan **10**, 842 (1955).
[5] R. L. Conger and F. C. Essig, Phys. Rev. **104**, 915 (1956).
[6] D. O. Smith, J. Appl. Phys. **29**, 264 (1958).
[7] See, for example, *Proceedings of the Conference on Magnetism and Magnetic Materials, Boston, October, 1956* (American Institute of Electrical Engineers, New York, 1957); also *Proceedings of the Conference on Magnetism and Magnetic Materials, Washington, D. C., November, 1957*, J. Appl. Phys. **29**, 237–548 (1958).
[8] H. R. Nelson, J. Chem. Phys. **5**, 252 (1937).

saturation magnetization is observed[9] and this decrease would then change the magnitude of the anisotropy. The films observed for this report are well within the range of thickness to possess "bulk" magnetic properties. Therefore, this oxide layer in no way effects the results of this particular investigation.

Under these conditions of evaporation the magnetic properties of the iron films are reproducible. The samples show the bulk value for saturation magnetization in iron of 1700 gauss.[10] Bozorth reports a value of 1714 gauss at 20°C for iron crystals. The value of 1700 gauss is well within the error of this investigation and is therefore used for the computations. The field necessary to saturate these specimens is about 45 oersteds. The magnitude of this field is affected by the conditions of preparation. Lower rates of evaporation, higher pressures, or dirty substrates increase the value of the field necessary for saturation significantly. Annealing of the specimens decreases the value to 20 oe or less.

EVAPORATION GEOMETRY

The methods of preparing the samples are similar to those discussed elsewhere[9,11] but will be repeated here briefly.

Figure 1 is a schematic drawing of the vacuum system showing the parts of most interest to this experiment. The tungsten evaporating filament is located in the bottom of the system in a five-sided copper box, 3.8 cm by 5 cm by 5 cm, which is water-cooled during an evaporation. Two specimens are deposited in each evaporation, a rate strip which monitors the thickness

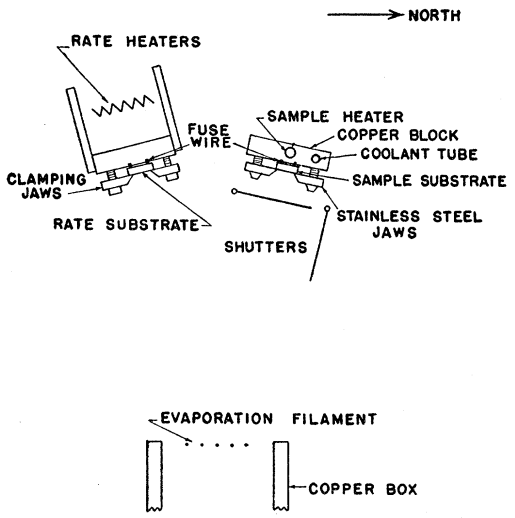

FIG. 1. Evaporation system viewed parallel to long dimension of sample.

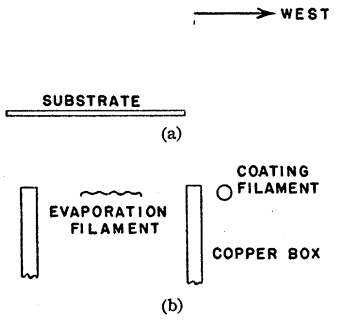

FIG. 2. Evaporation geometry viewed perpendicular to long dimension of sample.

and the sample whose thickness is controlled by a set of mechanical shutters. Each specimen is mounted in a furnace which allows temperature control of the substrate. The sample furnace is a copper block 0.7 cm by 2.3 cm by 6.4 cm through which two longitudinal holes are bored. Stainless steel tubing is inserted in the lower of these borings and used as support for the block as well as a path for coolants to the sample furnace. The other hole holds a 100-watt light bulb filament which serves as a source of heat to the block. The rate furnace can only be heated. This is accomplished by means of a set of coiled tungsten filaments. There are four coils wound in series electrically such that each pair produces magnetic fields in opposition. All heater currents are supplied by ac power including the current to the evaporation filaments.

The glass substrates are clamped into the furnaces by means of chamfered steel jaws which also define the width of the deposited specimens. The rate films are 0.39 cm in width while the sample films are 0.36 cm wide. The jaws holding the sample are a nonmagnetic stainless steel alloy. The other parts of the sample furnace are also nonmagnetic. This type of material is employed to minimize the effects of magnetic fields in the vicinity of the sample films. The substrates are backed into the furnaces with lead fuse wires to insure a good thermal path. With this clamping arrangement the temperature rise of a film and substrate during exposure to the hot filament has been shown to be less than one degree Centigrade using an annealed film as a resistance thermometer.

Both the rate and the sample furnace are tilted such that the flux of metallic vapor is normal to the glass substrate at the center of the film. However, since the deposited film is about 6 cm in length and the filaments are less than half that value, the lines of flux of the vapor near the ends of the film are considerably inclined with respect to a normal of the substrate (see Fig. 2). The distance from the evaporation filament to the sample substrate is 9.5 cm.

The tungsten filament incorporated in an evaporation is fabricated from 30-mil tungsten wire bent to produce a flat area of five "legs" which will eventually hold the iron charge. The "legs" are crinkled slightly to prevent

[9] E. C. Crittenden, Jr., and R. W. Hoffman, Revs. Modern Phys. **25**, 310 (1953).
[10] R. M. Bozorth, *Ferromagnetism* (D. Van Nostrand and Company, Inc., 1951), p. 867.
[11] H. S. Story and R. W. Hoffman, Proc. Phys. Soc. (London) **B70**, 950 (1957).

motion of the iron on the filament after it has melted. The "legs" are mounted parallel to the long dimension of the substrate. About 50 mg of No. 36 gauge, 99.9% pure iron wire is wound into a helical form and slipped over each of the five "legs" of the filament. The total charge is about 250 mg. With this charge and the filament design employed here, little alloying of the iron with the tungsten filament is observed in preparing samples in this thickness range. A new filament and charge is used for each sample.

A second tungsten filament, referred to as the coating filament, is located to the west side of the evaporating filament. It consists of a loose helix of 30-mil tungsten wire placed so an inactive coating can be evaporated onto a metallic film after deposition. The side wall of the filament box prevents cross transfer of material between the two filaments during depositions. A coating about 200 A thick is used to inhibit oxidation of the specimens: MgF_2 is used for iron films. Most of the films measured for this report were uncoated. However, the application of a MgF_2 coating did not influence the quality of the observed anisotropy in the iron specimens.

The samples used in this investigation were made with the glass substrates held at 75°C for comparison with other results obtained in this laboratory. The rate films were held at 200°C for reasons pertaining to thickness calibration. The films employed here are roughly of constant thickness with nominal variations ranging from 320 to 390 angstrom units. The character of the effect discussed is not affected by a change in film thickness. Iron films between 100 and 2500 A possess the same type of magnetic anisotropy as the films reported. Specimens outside this thickness range have not been measured.

MAGNETIC MEASUREMENTS AND INTERPRETATION

The magnetic measurements were made in the 60-cycle loop tracer discussed by Crittenden[12] and modified by Rosette. The H field was applied in the plane of the film and the magnetization was measured parallel to the applied H. Anisotropy is determined from magnetization curves obtained by plotting the tips of the B-H loops as the drive field is decreased. This is done in various directions and the difference in the area between magnetization curves in different directions is here designated as the magnetic anisotropy. This area is measured with a planimeter and multiplied by the appropriate calibration to determine the value of the anisotropy energy.

The specimen had to be cut because of limited space in the pickup coil and because the measurements were required in at least two directions. The measureable sample size was approximately a square 0.6 cm on a side. Thus, the resultant samples were smaller in dimension than the length of the pickup coil. The result is a saturation value of M less than the bulk value and a value of saturation which varies greatly with the sample size. The reason for this decrease in saturation is that some flux closure lines do not link the pickup coil due to the smaller size of the sample. Cutting the specimens to this size lowers the observed saturation but does not change the shape of the magnetization curves. Before cutting, long samples were measured and this saturation magnetization was compared with bulk. In all measured cases the value agreed with the 1700 gauss bulk iron value. The data for the small samples is, therefore, reported as normalized to the bulk saturation value of M. This eliminates any size effects and allows comparison of the results.

Preliminary investigations of domain walls in these specimens with the "Bitter technique" have shown relatively narrow cigar-shaped island-like domains. This shape of domain is in agreement with the observations of Williams[13] and others[14,15] on thin iron films. Stress in films[16] limits the possibility of domain wall motion.[17] With the presence of stress, the energy considerations are such that domain rotation is more favorable at lower fields. Magnetic saturation is observed in iron films at relatively low applied fields. Therefore, the resultant switching is most likely accomplished by a magnetic rotation process. This fact has been observed experimentally in other investigations.[1,5] Smith has calculated theoretical hysteresis-loops for films similar to those studied here.[6] The model consists of a thin ferromagnetic film, possessing uniaxial anisotropy, in which switching is accomplished by rotational processes only.

Magnetization curves can easily be inferred from Smith's hysteresis loops. A comparison between these

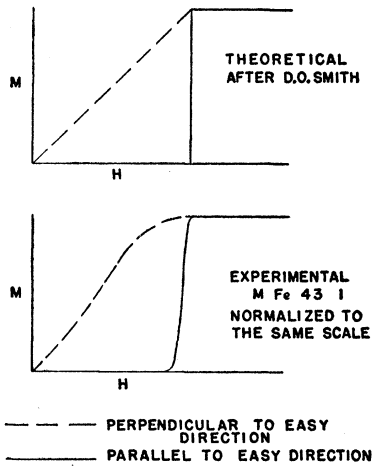

FIG. 3. Comparison of theoretical and experimental magnetization curves. The model considers only rotational switching in films with an uniaxial anisotropy.

[12] Crittenden, Hudimac, and Strough, Rev. Sci. Instr. **22**, 872 (1951).

[13] H. J. Williams and R. C. Sherwood, J. Appl. Phys. **28**, 548 (1957).

[14] T. Iwata and M. Yamamoto, Sci. Repts. Research Insts., Tohoku Univ. Ser. A**8**, 293 (1956).

[15] H. J. Williams and M. Goerty, J. Appl. Phys. **23**, 316 (1952).

[16] J. D. Finegan and R. W. Hoffman (to be published).

[17] K. H. Stewart, *Ferromagnetic Domains* (Cambridge University Press, New York, 1954).

magnetization curves and a typical set of experimental curves is shown in Fig. 3. The similarity in the character of these curves is the basis upon which the perpendicular direction in the film is termed the easy direction of magnetization and the parallel or long direction of the film is termed the hard direction. The similarity of these curves with the calculated curves also suggests that the rotational process is in effect. These are the extreme magnetization curves so the films investigated here do display uniaxial anisotropy in the plane of the film.

RESULTS

In general, magnetization curves were measured in two perpendicular directions, parallel and perpendicular to the long dimension of the evaporated specimens (hereafter referred to as $\parallel$ and $\perp$, respectively). This results in a set of *M versus H* curves as the measurements were made at various positions along the specimens. A typical set of curves is presented in Fig. 4. The solid curve is the $\perp$ direction while the dashed curve is the $\parallel$ direction. A single curve indicates that both directions coincide. The numbers designate location of the measured sample in the specimen. Number 1 is the east end, increasing to 10 at the west end. The area between these two magnetization curves is converted to a value of anisotropy and plotted as a function of film location; see Fig. 5. The location of the filament is indicated in the anisotropy plot by the heavy line on the abscissa.

The specimen shown in Figs. 4 and 5 is representative of the observed phenomenon. The film appears isotropic in the region directly over the filament and displays an increasing anisotropy toward both ends of the specimen. Measurements in directions other than $\parallel$ and $\perp$ yield magnetization curves that fall between these directions in the anisotropic regions of the specimens.

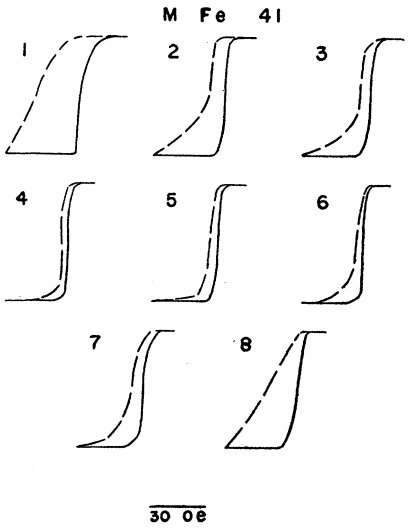

FIG. 4. Experimental magnetization curves (*M vs H*) at various locations along the length of the sample.

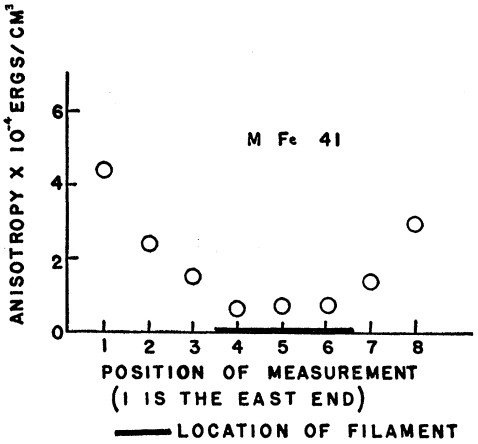

FIG. 5. Measured magnetic anisotropy at different locations along the length of the sample. The heavy line on the abscissa indicates the position of the evaporation filament.

Hence these directions are the extremes, the easiest direction of magnetization in the case of the $\perp$ measurements and the hardest direction in the case of the $\parallel$. In the isotropic region measurements in many directions result in magnetization curves that coincide with the $\parallel$ and $\perp$ curve, and every direction is equivalent. The specimen is, therefore, magnetically isotropic in this region.

A single condition of evaporation was changed at a time, to test its effect on the resulting anisotropy. The substrate glass was cut before the film was deposited to check any mechanical effect. The substrate of another specimen was not clamped in the furnace during deposition to eliminate any stresses induced in the clamping process. To check effects of stray magnetic fields, the sample heater was off during the time of one evaporation, the rate heaters during another, and both during a third. The evaporation filament was rotated in another deposition and in fact, changed to a helical coil with its axis vertical in still another. These changes checked all fields present except the field due to the wires leading into the evaporating filament and the earth's field. None of the above situations change the anisotropy configuration in any significant manner. A sample was made at a temperature of 200°C in the location of a rate specimen. The resultant magnetization curves showed a slight increase in the field necessary to saturate. Another specimen was annealed at 250°C in the vacuum system before removal. This decreased the anisotropy slightly. But again, neither of these changes affected the quality of the anisotropy configuration whatsoever.

The evaporating filament was then moved, first, below the west end of the substrate and then for another specimen, below the east end. The resulting anisotropy curves are presented in Fig. 6. The isotropic region of the specimen has moved to be directly over the filament. This eliminates the lead-in wires to the

evaporating filament as the possible cause of the effect. They remained constant during the evaporations listed above and the changes in anisotropy. The conclusion seems to be that the cause of the anisotropy is dependent on the location of the filament, or in other words, depends on the angle the incident flux of metallic vapor makes with a normal to the substrate. With normal incidence, the result is isotropy; with inclination of the vapor to the normal there results anisotropy.

An effect with similar geometric dependence is the formation of a fiber axis in thin evaporated films reported by Evans and Wilman,[18] and others.[8,19–21] Their observations show that as a film is formed by condensation from vapor, a fiber axis structure is developed. The fiber axis is inclined toward the direction of the arriving vapor stream but is not necessarily parallel to it. Fiber axes are even observed in iron films thinner than 100 A. In iron the fiber axis is a [111] crystallographic direction. Hence, the induced structure is such that [111] directions are inclined toward the evaporating filament while there is random orientation about this axis. Evans and Wilman also report that the tilt of the fiber axis starts from zero at normal incidence, reaches a maximum, and then decreases slightly as the angle of the vapor incidence continues to increase. These angles are measured with respect to a normal to the substrate. In the case of iron films evaporated on glass substrates, the maximum tilt of the fiber axis is about 10° at a vapor incidence of around 20°. Evans and Wilman have also observed that the rate of evaporation and the substrate roughness do not effect the formation of the fiber axis structure. Reflection electron diffraction patterns of several of the iron films used in the magnetic investigation show the same fiber axis structure observed by Evans and Wilman.

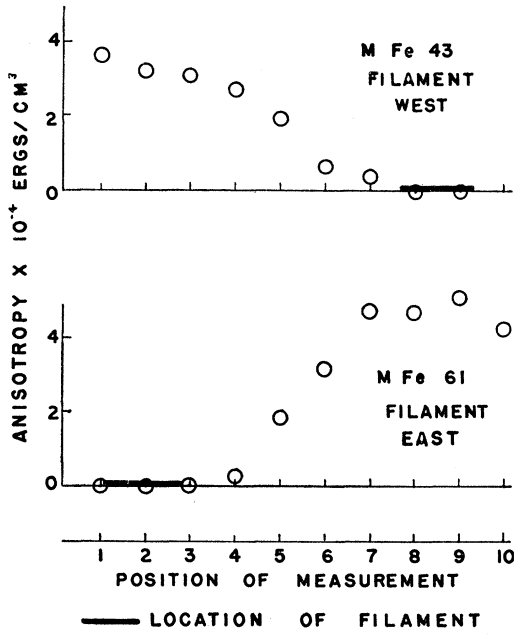

FIG. 6. Magnetic anisotropy *vs* position, showing effect of moving the evaporation filament.

The magnetic anisotropy in the plane of the film owing to this fiber axis structure can be calculated from the difference in energy necessary to saturate in the $\perp$ and $\parallel$ directions. For the details of this calculation see the appendix. The results of the calculation show an average anisotropy of 1.7×10^4 ergs/cm³ for iron with a 100% [111] fiber structure tilted 10°, with a skin stress of 8×10^9 dynes/cm². The average anisotropy is exactly zero at 0° tilt. An anisotropy in film stress has also been observed. Finegan and Hoffman[16] report a stress anisotropy in iron films prepared similarly to those reported here. The stress in the hard direction is about 17% lower than the stress in the easy direction, at the ends of the film. Applying this stress anisotropy to the calculation yields a value for the average anisotropy of 3×10^4 ergs/cm³ when the fiber axis structure is tilted 10°. The calculated values must also be modified by the amount of fiber axis orientation. Arcing on the electron diffraction plates suggests a very strong but incomplete fiber axis structure, perhaps about 75 to 90%. This would lower the calculated values somewhat. A higher temperature of evaporation would increase the percentage of fiber axis structure while annealing some of the imperfections. Annealing imperfections would lower the stress and thus lower the magnitude of the anisotropy. As listed above a specimen evaporated at 200°C displayed a slightly higher anisotropy. After annealing at elevated temperatures the anisotropy is observed to decrease significantly. Some of the specimens investigated displayed evidence of wall motion processes; in these the observed anisotropy is not expected to agree with the above calculation. All of the films studied, that show only rotational switching, have anisotropies which agree with the calculated values.

In general, the magnitude of the effects of these various conditions on the anisotropy are quite difficult to predict. The resulting calculated values should therefore be considered only as indicative of the anticipated experimental results. The magnitude of the stress anisotropy is correlated with the tilt of the fiber axis. Hence, the observed magnetic anisotropy should be describable in terms of the qualities of the fiber axis present in the iron specimens. This is indeed the situation. As the fiber axis becomes normal to the substrate the observed magnetic anisotropy becomes zero as is required by the calculation. The anisotropy becomes zero in this region even in specimens which display wall motion.

The only remaining consideration is the effect of the earth's field on the observed anisotropy. To test this,

[18] D. M. Evans and H. Wilman, Acta. Cryst. **5**, 731 (1952).
[19] G. I. Finch and A. G. Quarrell, Proc. Roy. Soc. (London) **A141**, 398 (1933).
[20] K. R. Dixit, Phil. Mag. **16**, 1049 (1933).
[21] S. Konobeevsky and J. Umansky, J. Phys. U.S.S.R. **10**, 388 (1946).

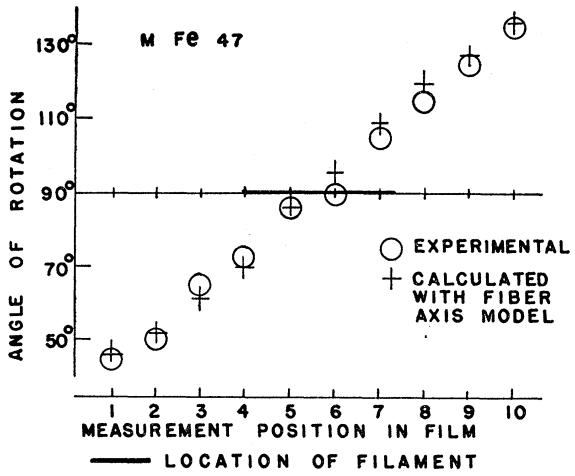

FIG. 7. Comparison of observed and calculated hard directions of magnetization in a film condensed on a substrate rotated 15° about an axis parallel to the long dimension.

a substrate was clamped into the sample furnace but tilted relative to the arriving flux of metal vapor. This was accomplished by modifying the fuse wires backing the glass substrate into the furnace. On one side the fuse wire was flattened while on the other side the thickness was doubled. The net effect was a tilt of about 15°, so the metal flux arrived inclined at this angle in the center area of the film. This resulted in a fiber axis structure which produces a hard direction of magnetization in the $\perp$ direction at the center of the specimen. Nearer the ends of the film the hard direction was in. neither the $\parallel$ nor $\perp$ direction but somewhere in between The change in location of the substrate was so slight that the field configuration due to the earth's field must have been effectively the same in the specimen region as in an untilted specimen.

Considering the fiber axis structure produced in this specimen, the location of the hard direction of magnetization was calculated and is shown as the crosses in Fig. 7. Angles are measured relative to the long dimension of the specimen, where 0° is the $\parallel$ direction of the film. The circles are the location of the hard direction as determined by observing magnetization curves in four different directions. The maximum anisotropy observable depends on the tilt of the fiber axis. As the fiber axis of this specimen had a tilt of about 9.5° in the center and about 10° near the ends (the direction of the tilt changes, of course) the largest observed value of anisotropy should increase slightly in moving from the center to the ends of the specimen. The anisotropy between the extreme magnetization curves in this tilted specimen was 6.6×10^4 ergs/cm^3 at the center and increased to 7.1×10^4 ergs/cm^3 at the ends of the film. Agreement of the data with the predicted results definitely indicates that the fiber axis structure was producing the anisotropy effect. The influence of the earth's field was apparently quite small, if not negligible.

Finch and Quarrell[19] have shown that exposure to a hot filament will produce fiber axis structure. They observed that a weak fiber axis could be enhanced by exposing the specimen to a hot filament. Also a completely unoriented specimen displayed a strong fiber axis structure after exposure to heat from a small filament. The filament they employed for this heating was the filament designed to discharge the specimen in their electron diffraction camera.

This effect of exposure to a hot filament has also been observed in the magnetic measurements made for this investigation. The resulting change in anisotropy can be explained by considering the fiber axis structure formed, not by a flux of metal vapor as such but, by a flux of energy which is incident on the substrate. As the angle of incidence of this energy varies, the fiber axis tilts in the same direction. For example, a region of isotropy near the east end of a film becomes anisotropic when exposed to heating provided by the coating filament which is below the west end of the specimens. The geometry of the anisotropy is exactly the same as that produced in regular deposition from the evaporating filament. The effect of heating from the coating filament is superimposed on the original anisotropy. The additional heat flux is apparently sufficient to reorient the fiber axis structure of the crystallites in the specimen.

CONCLUSIONS

The results of this investigation indicate that the formation of a magnetic anisotropy in thin evaporated iron films results from a fiber axis structure which developes as the specimen is being deposited. If the incident direction of metallic flux varies from the normal, the fiber axis tilts in a similar direction. As soon as this occurs a magnetic anisotropy is produced. An anisotropy of 3×10^4 ergs/cm^3 has been produced in regions of iron films without the use of applied magnetic fields either during the evaporation or during a subsequent "magnetic" anneal. It is not suggested that the application of such fields will not produce anisotropy, indeed, they will. The conclusion is that such fields are not necessary and might not necessarily be the factor causing the observed magnetic anisotropy in thin evaporated films. The earth's field clearly does not produce this anisotropy. The factor which is the significant cause of the observed anisotropy in films prepared without the application of large fields is the geometric variation of the metallic vapor or heat flux incident on the substrate.

ACKNOWLEDGMENT

The authors wish to thank Mr. K. H. Rosette for his modifications and maintenance of the magnetic loop tracer. This research was supported by the U. S. Atomic Energy Commission and the National Carbon Company. One of the authors, T. G. Knorr, is also indebted to the National Carbon Company for a fellowship during 1957–58.

APPENDIX. CALCULATION OF MAGNETIC ANISOTROPY DUE TO FIBER AXIS STRUCTURE

The fiber axis structure in iron can be represented by fixing a [111] direction of the body-centered cubic structure and allowing arbitrary rotation around this fixed direction. In the region of isotropy in the specimens, the fiber axis is normal to the substrate. In the region of anisotropy the fiber axis is tilted such that it has a component in the film only in the $\|$ direction. This component is $\sin\gamma$, where γ is the angle of tilt.

The energy necessary for saturation magnetization considering rotational processes only is given by Kittel[22]:

$$\begin{aligned} f=&K_1(\alpha_1^2\alpha_2^2+\alpha_2^2\alpha_3^2+\alpha_3^2\alpha_1^2)+K_2(\alpha_1^2\alpha_2^2\alpha_3^2)\\ &+B_1(\alpha_1^2e_{xx}+\alpha_2^2e_{yy}+\alpha_3^2e_{zz})\\ &+B_2(\alpha_1\alpha_2e_{xy}+\alpha_2\alpha_3e_{yz}+\alpha_3\alpha_1e_{zx})\\ &+\tfrac{1}{2}C_{11}(e_{xx}^2+e_{yy}^2+e_{zz}^2)+\tfrac{1}{2}C_{44}(e_{xy}^2+e_{yz}^2+e_{zy}^2)\\ &+C_{12}(e_{yy}e_{zz}+e_{zz}e_{xx}+e_{xx}e_{yy}), \end{aligned}$$

where K_1 and K_2 are the crystalline anisotropy constants. B_1 and B_2 are constants related to the magnetostriction constants, and the C's are the elastic constants. α_1, α_2, α_3 are the direction cosines of the saturation magnetization with respect to the crystallographic [100] axes. The e's are the strain components relative to the same axes. Anisotropy will be the difference in the energy as calculated for two directions of a specimen.

The method employed for the calculation is to establish a new coordinate system in the plane of the film, with x' as the $\perp$ direction, y', the $\|$ direction and z', normal to the film. α_1, α_2, α_3 are first transformed into a new coordinate system with its z axis parallel to a [111] direction. An arbitrary rotation, β, around the new z axis (the [111] direction) is then performed. A final rotation, γ, around the x axis resulting from this second rotation above, accounts for the tilt of the fiber axis. The complete transformation is

$$\begin{bmatrix}\alpha_1\\ \alpha_2\\ \alpha_3\end{bmatrix}=\begin{bmatrix}0.707 & -0.408 & 0.577\\ 0 & -0.816 & 0.577\\ -0.707 & -0.408 & 0.577\end{bmatrix}\begin{bmatrix}\cos\beta & \sin\beta & 0\\ -\sin\beta & \cos\beta & 0\\ 0 & 0 & 1\end{bmatrix}\begin{bmatrix}1 & 0 & 0\\ 0 & \cos\gamma & \sin\gamma\\ 0 & -\sin\gamma & \cos\gamma\end{bmatrix}\begin{bmatrix}\alpha_1'\\ \alpha_2'\\ \alpha_3'\end{bmatrix}.$$

As β is varied, holding γ fixed, the effect is precisely that of rotating a crystal around its [111] direction, which is tilted the fixed angle γ. The transformation can be put in the form:

$$\begin{bmatrix}x\\ y\\ z\end{bmatrix}=\begin{bmatrix}l_1 & l_2 & l_3\\ m_1 & m_2 & m_3\\ n_1 & n_2 & n_3\end{bmatrix}\begin{bmatrix}x'\\ y'\\ z'\end{bmatrix},$$

where, for example, l_1, l_2, l_3 are the direction cosines between the x axis and x', y', z', respectively.

The e's must also be calculated from constants in the new system. Here the known quantity is a skin stress applied in the primed system, which is the plane of the film. The stress considered is of the form $X_x'\neq 0$, $Y_y'\neq 0$, with all other components equal to zero. The resulting expressions for the unprimed stress components are

$$\begin{aligned} X_x&=l_1^2X_x'+l_2^2Y_y'=a,\\ Y_y&=m_1^2X_x'+m_2^2Y_y'=b,\\ Z_z&=n_1^2X_x'+n_2^2Y_y'=c,\\ Y_z&=m_1n_1X_x'+m_2n_2Y_y'=u,\\ Z_x&=n_1l_1X_x'+n_2l_2Y_y'=v,\\ X_y&=l_1m_1X_x'+l_2m_2Y_y'=w. \end{aligned}$$

The stress components can be given in terms of the strains and reduced by the application of the cubic symmetry. The strain components are then determined from these expressions.

The calculation can now be performed. A plot of $f(\perp)-f(\|)$ *versus* β for iron is shown in Fig. 8. Owing to the threefold symmetry about a [111] direction in the cubic system, the function repeats itself every 120°. The constants for the calculation displayed in Fig. 8 are as follows:

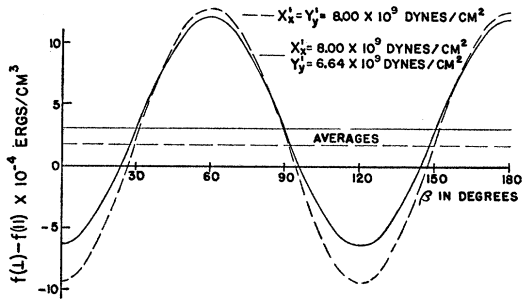

FIG. 8. Calculated magnetic anisotropy in iron films with a fiber axis tilted 10° from the normal to the plane of the film. Both isotropic and anisotropic stresses are shown.

$$\begin{aligned} K_1&=450\times10^3 \text{ ergs/cm}^3 \text{ at } 20^\circ\text{C},\\ K_2&=200\times10^3 \text{ ergs/cm}^3 \text{ at } 20^\circ\text{C},\\ B_1&=-2.9\times10^7 \text{ ergs/cm}^3,\\ B_2&=6.4\times10^7 \text{ ergs/cm}^3,\\ C_{11}&=2.29\times10^{12} \text{ dynes/cm}^2,\\ C_{44}&=1.14\times10^{12} \text{ dynes/cm}^2,\\ C_{12}&=1.34\times10^{12} \text{ dynes/cm}^2,\\ \gamma&=10^\circ,\\ X_x'&=8.00\times10^9 \text{ dynes/cm}^2,\\ Y_y'&=6.64\times10^9 \text{ dynes/cm}^2. \end{aligned}$$

[22] C. Kittel, Revs. Modern Phys. **21**, 541 (1949).

The function is calculated in 10° intervals of β and averaged. K_1 and K_2 are taken from Bozorth[10]; B_1 and B_2, from Kittel.[22] C_{11}, C_{12}, and C_{44} have been measured in this laboratory by Daniels.[23]

An isotropic skin stress of 8×10^9 dynes/cm^2 in iron would yield an average anisotropy of 1.7×10^4 ergs/cm^3 for a fiber axis tilt of 10°. The variation of $f(\perp)-f(\|)$ with β for the condition of isotropic stress is also shown in Fig. 8.

The anisotropy goes roughly as the sine^2 of the angle of tilt. The function $f(\perp)-f(\|)$ averages exactly to zero at a zero angle of tilt; this corresponds to the isotropy produced by normal incidence.

[23] W. B. Daniels, M.S. thesis, Case Institute of Technology, 1955 (unpublished).

PHYSICAL REVIEW VOLUME 113, NUMBER 4 FEBRUARY 15, 1959

Model for Lattice Thermal Conductivity at Low Temperatures

JOSEPH CALLAWAY
Westinghouse Research Laboratories, Pittsburgh, Pennsylvania

(Received October 10, 1958)

A phenomenological model is developed to facilitate calculation of lattice thermal conductivities at low temperatures. It is assumed that the phonon scattering processes can be represented by frequency-dependent relaxation times. Isotropy and absence of dispersion in the crystal vibration spectrum are assumed. No distinction is made between longitudinal and transverse phonons. The assumed scattering mechanisms are (1) point impurities (isotopes), (2) normal three-phonon processes, (3) umklapp processes, and (4) boundary scattering. A special investigation is made of the role of the normal processes which conserve the total crystal momentum and a formula is derived from the Boltzmann equation which gives their contribution to the conductivity. The relaxation time for the normal three-phonon processes is taken to be that calculated by Herring for longitudinal modes in cubic materials. The model predicts for germanium a thermal conductivity roughly proportional to $T^{-\frac{1}{2}}$ in normal material, but proportional to T^{-2} in single-isotope material in the temperature range 50°–100°K. Magnitudes of the relaxation times are estimated from the experimental data. The thermal conductivity of germanium is calculated by numerical integration for the temperature range 2–100°K. The results are in reasonably good agreement with the experimental results for normal and for single-isotope material.

INTRODUCTION

ALTHOUGH an exact calculation of lattice thermal conductivity is possible in principle, lack of knowledge of crystal vibration spectra and of anharmonic forces in crystals and the difficulty of obtaining exact solutions of the Boltzmann equation are formidable barriers to progress. It is interesting to investigate the consequences of a simple model which is more amenable to calculation. It is assumed in this work that all the phonon scattering processes can be represented by relaxation times which are functions of frequency and temperature. It is further assumed that the material is elastically isotropic and dispersion in the vibrational spectrum is neglected. As a small concession to reality, the relaxation time for normal three phonon processes is taken to be that characteristic of longitudinal modes in a cubic crystal.[1] No distinction is made between longitudinal and transverse phonons.

It is well known that normal processes (scattering processes which conserve the total crystal momentum) cannot by themselves lead to a finite thermal conductivity.[2] Consequently, it cannot be legitimate just to add reciprocal relaxation times for the normal processes (N processes) to those which do not conserve the crystal momentum. Examples of the latter type of process include umklapp processes, impurity scattering, and boundary scattering (we shall designate all such momentum-destroying processes as U processes). U processes tend to return the phonon system to an equilibrium Planck distribution, whereas N processes lead to a displaced planck distribution. An investigation of this point is made in some detail to allow the effect of normal processes to be included more exactly.

Existence of the following scattering processes is assumed: (1) Boundary scattering, described by a constant relaxation time L/c, where c is the velocity of sound and L is some length characteristic of the material. (2) Normal three-phonon processes whose relaxation time is taken to be proportional to $(\omega^2T^3)^{-1}$, where ω is the circular frequency and T is the absolute temperature. For further discussion of this choice, see the Appendix. (3) Impurity scattering, including isotope scattering, whose relaxation time is independent of temperature and proportional to ω^{-4}. (4) Umklapp processes with a relaxation time proportional to $(e^{-\Theta/aT}\omega^2T^3)^{-1}$, where Θ is the Debye temperature and a is a constant characteristic of the vibrational spectrum

[1] C. Herring, Phys. Rev. **95**, 954 (1954).
[2] R. E. Peierls, *Quantum Theory of Solids* (Oxford University Press, Oxford, 1955), Chap. 2.